Drug Resistance Updates 73 (2024) 101054

Contents lists available at ScienceDirect

Drug Resistance Updates

journal homepage: www.elsevier.com/locate/drup

Inhibition of SIRT7 overcomes sorafenib acquired resistance by suppressing ERK1/2 phosphorylation via the DDX3X-mediated NLRP3 inflammasome in hepatocellular carcinoma

Yuna Kim [a,*,1], Kwan-Young Jung [b,1], Yun Hak Kim [c,d,1], Pan Xu [e], Baeki E. Kang [a], Yunju Jo [f], Navin Pandit [b], Jeongho Kwon [a], Karim Gariani [g], Joanna Gariani [h], Junguee Lee [i], Jef Verbeek [j,k], Seungyoon Nam [l,m], Sung-Jin Bae [n], Ki-Tae Ha [o], Hyon-Seung Yi [p], Minho Shong [q], Kyun-Hwan Kim [a], Doyoun Kim [b], Hee Jung Jung [b], Chang-Woo Lee [a], Kwang Rok Kim [b,**], Kristina Schoonjans [e,****], Johan Auwerx [e,****], Dongryeol Ryu [a,f,***]

[a] Department of Molecular Cell Biology, Sungkyunkwan University School of Medicine, Suwon, Republic of Korea
[b] Therapeutics & Biotechnology Division, Korea Research Institute of Chemical Technology, Daejeon, Republic of Korea
[c] Department of Anatomy, School of Medicine, Pusan National University, Yangsan, Republic of Korea
[d] Department of Biomedical Informatics, School of Medicine, Pusan National University, Yangsan, Republic of Korea
[e] Laboratory of Integrative Systems Physiology, Institute of Bioengineering, Ecole Polytechnique Federale de Lausanne, Lausanne, Switzerland
[f] Department of Biomedical Science and Engineering, Gwangju Institute of Science and Technology, Gwangju, Republic of Korea
[g] Service of Endocrinology, Diabetes, Nutrition and Therapeutic Patient Education, Geneva University Hospitals, Geneva, Switzerland
[h] Department of radiology, Hirslanden Grangettes Clinic, Geneva, Switzerland
[i] Department of Pathology, Daejeon St. Mary's Hospital, College of Medicine, The Catholic University of Korea, Daejeon, Republic of Korea
[j] Laboratory of Hepatology, Department of Chronic Diseases and Metabolism (CHROMETA), KU Leuven, Belgium
[k] Department of Gastroenterology and Hepatology, University Hospitals KU Leuven, Leuven, Belgium
[l] Department of Genome Medicine and Science, AI Convergence Center for Medical Science, Gachon Institute of Genome Medicine and Science, Gachon University Gil Medical Center, Gachon University College of Medicine, Incheon, Republic of Korea
[m] Department of Health Sciences and Technology, Gachon Advanced Institute for Health Sciences and Technology (GAIHST), Republic of Korea
[n] Department of Molecular Biology and Immunology, Kosin University College of Medicine, Busan, Republic of Korea
[o] Department of Korean Medical Science, Pusan National University School of Korean Medicine, Yangsan, Republic of Korea
[p] Laboratory of Endocrinology and Immune System, Chungnam National University School of Medicine, Daejeon, Republic of Korea
[q] Research Center for Endocrine and Metabolic Diseases, Chungnam National University School of Medicine, Daejeon, Republic of Korea

ARTICLE INFO

Keywords:
Hepatocellular carcinoma
Sorafenib resistance
SIRT7 inhibitor
ERK1/2 phosphorylation
DDX3X

ABSTRACT

Aims: Sirtuin 7 (SIRT7) plays an important role in tumor development, and has been characterized as a potent regulator of cellular stress. However, the effect of SIRT7 on sorafenib acquired resistance remains unclear and a possible anti-tumor mechanism beyond this process in HCC has not been clarified. We examined the therapeutic potential of SIRT7 and determined whether it functions synergistically with sorafenib to overcome chemoresistance.

Abbreviations: CHX, cycloheximide; DMEM, Dulbecco's Modified Eagle Medium (DMEM); DTT, dithiothreitol; eIF2α, eukaryotic initiation factor 2α; ERK1/2, extracellular signaling-regulated kinase1/2; FBS, fetal bovine serum; GSEA, gene set enrichment analysis; LC-MS/MS, liquid chromatography with tandem mass spectrometry; LIHC, liver hepatocellular carcinoma; MTT, 3-[4,5-dimethylthiazol-2-yl]− 2,5 diphenyl tetrazolium bromide; pERK1/2, phosphorylated ERK1/2; RIPA, radioimmunoprecipitation assay; SG, stress granule; shRNA, short-hairpin RNA; TCGA, The Cancer Genome Atlas; WT, wild-type.

* Correspondence to: Department of Molecular Cell Biology Sungkyunkwan University School of Medicine Suwon, 16419, Republic of Korea.
** Correspondence to : Therapeutics & Biotechnology Division, Korea Research Institute of Chemical Technology, Daejeon 34114, Republic of Korea.
*** Correspondence to: Department of Biomedical Science and Engineering Gwangju Institute of Science and Technology, Gwangju 61005, Republic of Korea.
**** Correspondence to: Laboratory of Integrative Systems Physiology Institute of Bioengineering, School of Life Sciences Ecole Polytechnique Federale de Lausanne, Lausanne CH-1015, Switzerland.
E-mail addresses: yuna716@skku.edu (Y. Kim), kkrok@krict.re.kr (K.R. Kim), kristina.schoonjans@epfl.ch (K. Schoonjans), admin.auwerx@epfl.ch (J. Auwerx), dryu@gist.ac.kr (D. Ryu).
[1] These authors contributed equally to this work.

https://doi.org/10.1016/j.drup.2024.101054
Received 7 September 2023; Received in revised form 10 December 2023; Accepted 11 January 2024
Available online 17 January 2024

Methods: Cancer Genome Atlas-liver HCC data and unbiased gene set enrichment analyses were used to identify SIRT7 as a potential effector molecule in sorafenib acquired resistance. Two types of SIRT7 chemical inhibitors were developed to evaluate its therapeutic properties when synergized with sorafenib. Mass spectrometry was performed to discover a direct target of SIRT7, DDX3X, and DDX3X deacetylation levels and protein stability were explored. Moreover, an in vivo xenograft model was used to confirm anti-tumor effect of SIRT7 and DDX3X chemical inhibitors combined with sorafenib.
Results: SIRT7 inhibition mediated DDX3X depletion can re-sensitize acquired sorafenib resistance by disrupting NLRP3 inflammasome assembly, finally suppressing hyperactive ERK1/2 signaling in response to NLRP3 inflammasome-mediated IL-1β inhibition.
Conclusions: SIRT7 is responsible for sorafenib acquired resistance, and its inhibition would be beneficial when combined with sorafenib by suppressing hyperactive pro-cell survival ERK1/2 signaling.

Introduction

HCC is the sixth most common malignancy and fourth most common cause of cancer-related deaths globally (Bray et al., 2018). The 5-year survival rate for advanced hepatocellular carcinoma (HCC) is < 2%, which is the lowest among all solid tumors (Siegel et al., 2019). However, only a limited number of patients will benefit from HCC therapy, which significantly hinders its application. Therefore, more comprehensive therapeutic approaches to enhance the therapeutic effect of blockade of current HCC treatment should be reconsidered to empower individuals to effect positive outcome (Liu et al., 2023; Picard and Do, 2022).

Sorafenib is a multikinase inhibitor that mainly targets kinase activity in the RAF/MEK/ERK signaling pathway, which is heavily involved in tumor invasion and metastasis in HCC. Despite efforts to develop clinically effective strategies for targeting HCC (Yang et al., 2023; Zhao et al., 2023), sorafenib has remained a globally accepted first-line systemic therapy for HCC for over a decade. However, sorafenib acquired resistance has become an obstacle to extending the overall survival benefits to patients with HCC (Bruix et al., 2021; Llovet et al., 2008). The heterogeneity of HCC often limits the respond and survival rate and make difficult to identify driver genes that can effectively attenuate HCC progression. Consequently, HCC remains one of the most challenging cancers to treat.

Phosphorylated ERK1/2 (pERK1/2) is a well-known downstream component of the RAF/MEK/ERK signaling cascade, which reflects the level of pathway activation in tumor tissues. pERK1/2 levels increase stepwise in accordance with the metastatic potential of HCC cells (Reddy et al., 2003; Zhang et al., 2009) and pERK levels have been proposed to predict the response of HCC cells to sorafenib (Llovet et al., 2012). However, this remains a clinically controversial issue (Chen et al., 2013; Negri et al., 2015; Personeni et al., 2013; Zhang et al., 2009), and its efficacy as a prognostic biomarker for sorafenib acquired resistance remains unclear.

The Cancer Genome Atlas (TCGA) suggests that SIRT7 expression is strongly correlated with the development of various types of cancer (Gong et al., 2018; Li et al., 2018; Wei et al., 2017). SIRT7, the least studied sirtuin family member, is a potent regulator of cellular stress and is important in the development of antitumor therapies (Ianni et al., 2021; Vakhrusheva et al., 2008). In human HCC, SIRT7 expression is up-regulated in a large cohort of patients (Kim et al., 2013; Zhao et al., 2019) and SIRT7 has been reported to induce ERK1/2 phosphorylation (pERK1/2) and activate the RAF/MEK/ERK signaling pathway to promote cancer cell proliferation (Yu et al., 2014). However, little is known regarding the biological functions of SIRT7 in chemoresistance and its association with pERK1/2 activation in sorafenib acquired resistant HCC.

Recently, combination therapy with atezolizumab and bevacizumab was identified for the treatment of treatment-resistant HCC. This therapy inhibits tumor growth and increases survival beyond that achieved with individual components alone (Finn et al., 2020; Shigeta et al., 2020). Therefore, we investigated the therapeutic potential of SIRT7 in sorafenib-resistant HCC and determined whether it works synergistically with sorafenib to mediate ERK1/2 signaling and influence the resistance mechanism.

Materials and methods

Cell lines

The human HCC cell lines Huh7 and SK-Hep1 were purchased from the Korean Cell Line Bank (KCLB, Korea). The human embryonic kidney cell line, HEK293T, was obtained from the American Type Culture Collection (ATCC). Cells were cultured in Dulbecco's modified Eagle's medium (DMEM) with 10% fetal bovine serum (FBS) and 1% penicillin/streptomycin in a humidified incubator at 5% CO_2 and 37 °C. Sorafenib-resistant Huh7^{SR} and SK-Hep1^{SR} cells were kindly provided by Prof. Keun-Gyu Park (Kyungpook National University, Korea) and were further generated by gradient exposed to sorafenib for approximately six months to acquire resistance (Byun et al., 2022).

Mouse models

All mice were treated according to the protocols reviewed and approved by the Institutional Animal Care and Use Committee (IACUC) of Sungkyunkwan University School of Medicine (SUSM) (code/SKKUIACUC 2021–07-47–1, approval date 20 Aug 2021). SUSM is an Association for the Assessment and Accreditation of Laboratory Animal Care International (No. 001004)-accredited facility. All experimental procedures were performed at Sungkyunkwan University in accordance with the regulations of the IACUC guidelines. BALB/c nude mice (5- to 6-week-old male Charles River) were used for xenograft experiments.

Cell-proliferation assay

Sorafenib-resistant and parental cells were seeded at a density of 5000 cells/well in 96-well plates. Briefly, an equal number of cells were treated with various concentrations of sorafenib, SIRT7 inhibitor (SIRT7i) #1 (Kim et al., 2019) and SIRT7i #2, which were gifted by Dr. Kwan-Young Jung, either alone or in combination. Cell viability was determined by 3-[4,5-dimethylthiazol-2-yl]− 2,5 diphenyl tetrazolium bromide (MTT) assay after 3 days of incubation, and cell numbers were calculated by trypan blue exclusion assay on the indicated days thereafter.

Colony-formation assay

Cells were seeded in 12-well plates (10,000 cells/well) and cultured in the presence of the indicated drugs. The cell colonies were then washed with PBS, fixed with a 1:3 ratio of acetic acid to methanol, and stained with crystal violet (Sigma-Aldrich, USA).

Plasmids and shRNA retroviral transduction

Oligonucleotides were synthesized and cloned into the pSIREN-RetroQ retroviral short hairpin RNA (shRNA) expression vector (Clontech, Takara Bio, Japan). Thereafter, pSIREN-RetroQ-Sirt7 and the negative-control vector (pSIREN-RetroQ) were transfected into HEK293T cells using PEI transfection reagent. pSIREN-RetroQ-Sirt7 and the negative-control vector (pSIREN-RetroQ) were gifts from Prof. Kazuya Yamagata (Kumamoto University, Kumamoto, Japan) (Fukuda et al., 2018). Subsequently, sorafenib-resistant HCC cells were infected with retroviral supernatant containing 8 μg/mL polybrene. After 24 h of incubation, the supernatant was replaced with medium containing 2 μg/mL puromycin. After 48 h, the virus-transduced cell lines were selected for further analysis.

Mass-spectrometry analysis

Gel lanes were cut into sections and subjected to in-gel digestion using end proteinase. The peptide digests were resuspended and analyzed by nano-liquid chromatography with tandem mass spectrometry (nano-LC-MS/MS) using an Orbitrap Elite Mass Spectrometer (BRE725600, Thermo Fischer Scientific, Texas, USA) coupled with an ultra-performance LC system (Ultimate 3000 RSLC, Thermo Fischer Scientific, Texas, USA). Data analysis was performed using Proteome Discoverer (v. 1.3, Protein Metrics, CA, USA).

Site-directed mutagenesis

The DDX3X expression plasmid cloned by PCR into the pcDNA3.1(+) vector using *Hin*dIII and *Xho*I restriction enzyme sites was a gift from Dr. Kyun-Hwan Kim (Sungkyunkwan University, Korea) (Park et al., 2019). The Muta-Direct™ Site-Directed Mutagenesis Kit (15071, INtRON Biotechnology, Inc., Seongnam, Korea) was used to generate the DDX3X site-directed mutant according to the manufacturer's instructions. Briefly, PCR was performed for mutagenesis using the wild-type (WT) DDX3X plasmid as a template. Mutant and WT DDX3X plasmids were transformed into XL-10 GOLD cells (200314, Agilent, CA, USA). All plasmids were confirmed by DNA sequencing.

In vitro acetylation and deacetylation assays

In vitro acetylation and deacetylation assays were performed as previously described (Rothgiesser et al., 2010; Ryu et al., 2014b). Briefly, 1 mg of recombinant DDX3X protein was incubated with 500 ng of recombinant p300 in acetylation buffer (50 mM Tris-HCl [pH 8], 100 mM NaCl, 10% glycerol, 1 mM phenylmethylsulfonyl fluoride, 1 mM dithiothreitol [DTT], 1 mg/mL bepstatin, 1 mg/mL leupeptin, 1 mg/mL pepstatin, 1 mM sodium butyrate, and 150 mM acetyl-CoA) for 1 h at 37 °C. After incubation, the samples were resolved by sodium dodecyl sulfate-polyacrylamide gel electrophoresis and analyzed by western blotting or in vitro deacetylation assays. For these assays, 1 mg of acetylated DDX3X was incubated with 500 ng of recombinant SIRT7 protein in deacetylation buffer (50 mM Tris-HCl [pH 9], 4 mM $MgCl_2$, 0.2 mM DTT, 1 mg/mL bepstatin, 1 mg/mL leupeptin, 1 mg/mL pepstatin, and 1 mM NAD^+) for 30 min with constant agitation. The incubated samples were resolved by SDS-PAGE and analyzed using western blotting or mass spectrometry. Recombinant p300 and SIRT7 proteins were kindly provided by Michael O. Hottiger (University of Zurich, Germany).

Immunoprecipitation assay

Cells were harvested in immunoprecipitation buffer (20 mM HEPES pH 7.9, 200 mM NaCl, 0.5 mM EDTA, 10% glycerol, 0.2% NP-40) containing phosphatase and protease inhibitors (Sigma) and were lysed for 30 min at 4 °C. The lysate was cleared by two sequential centrifugation steps. HA-coupled magnetic beads or agarose beads were used and were incubated overnight at 4 °C on a rotating wheel. The pull-down was eluted from the beads in 2 × Laemmli sample buffer (20 mM Tris pH 6.8, 4% SDS, 0.02% bromophenol blue, 13.4% glycerol, 2% β-mercaptoethanol) at 95 °C for 5 min. The samples were then analyzed by immunoblotting.

Immunofluorescence assay

Cells were grown in a slide chamber and treated with shControl, shSIRT7, DDX3X/WT, and DDX3X/55Q plasmids along with sorafenib, as described above. Treated cells were washed with PBS following a previously reported protocol (Pina et al., 2022). Cells were incubated with anti-G3BP1, anti-NLRP3, and anti-ASC antibodies and Alexa Fluor 488-conjugated mouse or Alexa Fluor 568-conjugated rabbit antibodies. DAPI-mounted cells were analyzed using CLSM (TSC SP8, Leica, Wetzlar, Germany), and images of the cells were obtained using LAS X software (LAS X office 1.4.5, Leica, Wetzlar, Germany).

Protein lysate preparation and western blotting

Cells were washed three times with PBS and lysed with radioimmunoprecipitation assay (RIPA) buffer (20 mM Tris-HCl pH 7.5, 150 mM NaCl, 1 mM EDTA, 1% NP-40, 1% sodium deoxycholate, 1 mM Na_3VO_4, and 1 mM NaF) supplemented with Complete Protease Inhibitor (Roche) and phosphatase inhibitor cocktails II and III (Sigma-Aldrich, USA). Protein concentration in the supernatant was quantified using a *DC* protein assay kit (Bio-Rad). Equal amounts of total proteins (20 μg) were separated by SDS-PAGE, transferred to a 0.45 mm Immobilon-P PVDF Membrane (Millipore, Merck, Germany), and incubated with primary antibodies overnight at 4 °C. After incubation with HRP-conjugated α-rabbit or α-mouse secondary antibodies for 1 h at room temperature (23–25 °C), the target protein bands were detected using a chemiluminescent detection reagent for 5 min and visualized using an imaging system (FUSION Solo S, VILBER, Eberhardzell, Germany).

Isolation of RNA and qRT-PCR

Total RNA was extracted using TRIzol Reagent (Invitrogen, USA) and reverse-transcribed into complementary DNA using a random hexamer primer (Thermo Fisher Scientific, USA). qRT-PCR was performed in triplicate using a QuantStudio 6 Flex Real-Time PCR System (Applied Biosystems, USA) according to the manufacturer's instructions.

RNA sequencing

Total RNA was prepared using the TRIzol method and the size of the PCR-enriched fragments, together with the template size distribution, was verified using an Agilent Technologies 2100 Bioanalyzer with a DNA 1000 chip (Agilent, CA, USA). Next-generation sequencing was performed using a HiSeq system according to the manufacturer's instructions (Illumina, San Diego, CA, USA). The sequences were processed and analyzed by Macrogen (Seoul, Korea).

Mouse xenografts–SIRT7i treatment with sorafenib

$Huh7^{SR}$ (5×10^6 cells per mouse) cells were injected subcutaneously into the right posterior flank of 5-week-old BALB/c nude mice (males, 5–6 mice per group). Tumor volume was calculated based on digital caliper measurements using a modified ellipsoidal formula: tumor volume = ½ length × $width^2$. After tumor establishment, mice were randomly assigned to 5 days per week of treatment with vehicle, sorafenib (15 mg kg^{-1}, oral gavage), SIRT7i #1 (5 mg kg^{-1}, oral gavage), SIRT7i #2 (2.5 mg kg^{-1}, oral gavage), or a drug combination in which each compound was administered at the same dose and schedule as the

single agent. Sorafenib and the two SIRT7 inhibitors were dissolved in ethanol and Cremophor EL/95% (50:50) to prepare a stock solution (4 ×), which was diluted in sterile water to obtain the final concentration prior to use.

Mouse xenografts–DDX3Xi (RK-33) treatment with sorafenib

Nude mice were injected in the flank with SK-Hep1^{SR} (2.5×10^6 cells per mouse) cells mixed with Matrigel. Mice were randomly distributed into three groups: DMSO as a control, sorafenib (15 mg kg^{-1}, oral gavage), and a combination of RK-33 (15 mg kg^{-1}, intraperitoneal) and sorafenib (15 mg kg^{-1}, oral gavage). Mice were treated with RK-33 once every 3 days for 3 weeks.

Immunohistochemical staining

Tumor tissues were fixed, embedded, and sliced into 5 μm-thick sections. Briefly, the paraffin sections were deparaffinized and hydrated. After microwave antigen retrieval, endogenous peroxidase activity was blocked by incubating the slides with 0.3% H_2O_2 and nonspecific

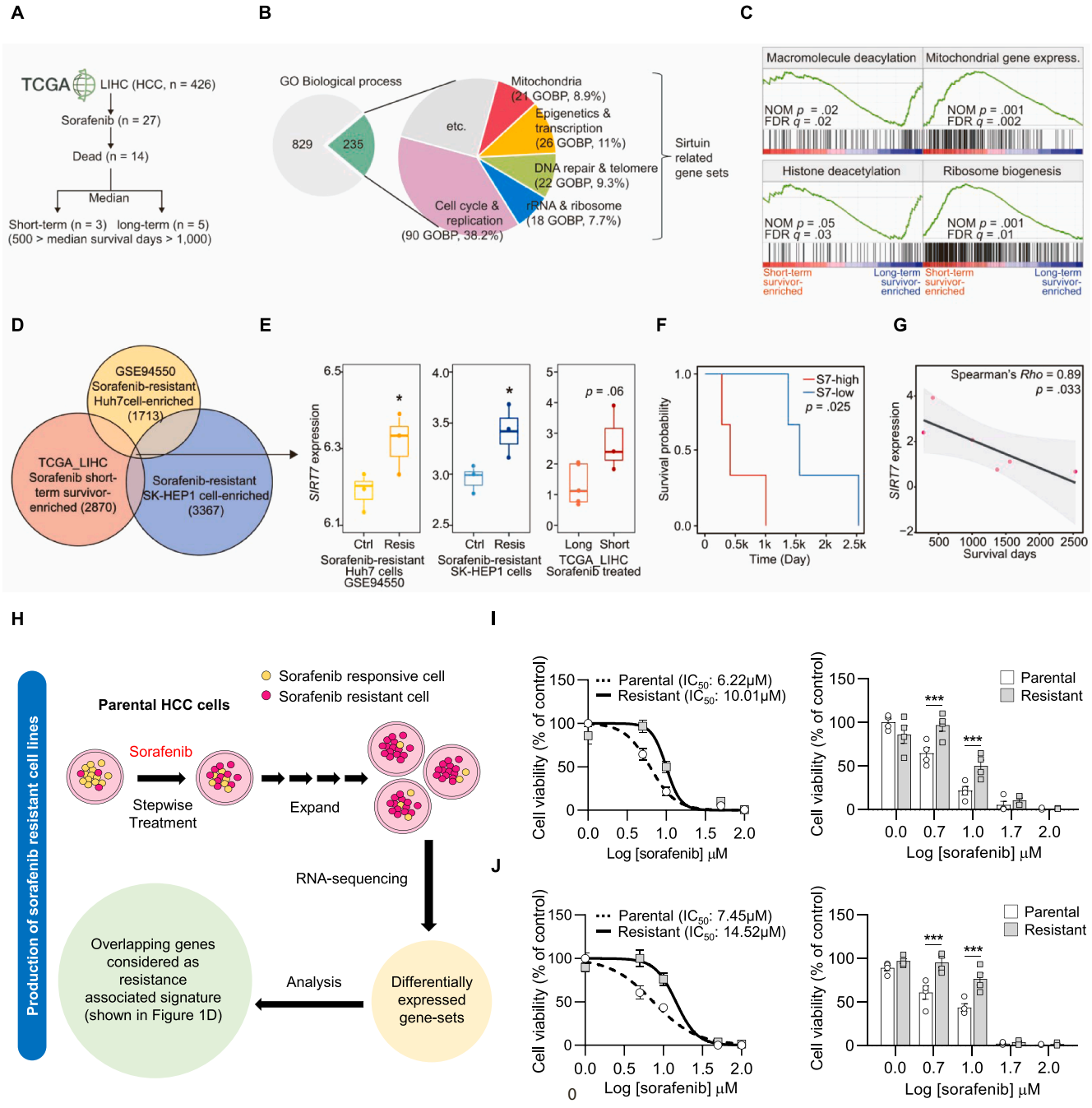

Fig. 1. Association analysis of the transcriptional expressions in sorafenib-resistant HCC samples. (A) Workflow of data selection. (B) Pie charts highlighting GSEA selected gene sets. (C) Enrichment plots of GSEA in sorafenib-received short-term survivors. (D and E) Venn diagram (D) showing RNA expression of sorafenib-received short-term survivors, Huh7^{SR} (GSE94550), and SK-Hep1^{SR} cells with box plots (E) presenting SIRT7 expression. (F and G) Line graphs showing the survival probability (F) and correlation (G) between hepatic SIRT7 and survival days. (H) Schematic image of production of sorafenib-resistant cell lines (I and J) Relative cell viability of Huh7^{SR} (I), SK-Hep1^{SR} (J) with their parental cells treated with sorafenib analyzed using an MTT assay. Data are represented as the mean ± SEM. Statistical analysis was conducted using a two-way ANOVA or two-tailed student's t-test, where appropriate, * $P < 0.05$; * * $P < 0.01$; * ** $P < 0.001$.

binding sites were blocked with 10% goat serum. Thereafter, the sections were incubated with primary antibodies (mouse anti-Ki-67and mouse anti-AFP) overnight at 4 °C, followed by incubation with horseradish peroxidase-conjugated secondary antibodies for 1 h at room temperature (23–25 °C). Finally, the sections were developed in diaminobenzidine solution under a microscope and counterstained with hematoxylin. The proliferation index was determined as the number of Ki-67- or AFP-positive cells/total number of cells in five randomly selected high-power fields (magnification ×200) using the ImageJ software (v. 1.46 r, NIH, MD, USA).

Statistical analysis

For analyses involving multiple comparisons, one-way ANOVA with Bonferroni post-hoc test was used. The student's t-test was used. Bar graphs show the mean ± SEM unless otherwise stated in the figure legend. All graphs were plotted and analyzed using GraphPad Prism 8 software. Statistical significance was set at $P < 0.05$.

Data and code availability

RNA sequencing and TCGA data were deposited in NCBI Gene Expression Omnibus (GEO: GSE94550). All the other datasets generated in this study are available from the corresponding authors upon request.

Results

TCGA liver HCC data implied that SIRT7 expression may be associated with sorafenib resistance

To identify candidates that potentially contribute to sorafenib-resistant HCC, TCGA-liver HCC (LIHC) data were analyzed, and the datasets were selected based on sorafenib-treated patients who survived for more than 1000 days or died within 500 days and who might have had sorafenib resistance (Fig. 1A). Unbiased gene set enrichment analysis (GSEA) was conducted to identify the sorafenib-sensitive or resistance-associated gene sets. Among the 1064 gene sets that belonged to the biological process Gene Ontology term, GSEA indicated that 235 gene sets qualified statistically (Fig. 1B). Among the 235 selected GSEA gene sets, 75.1% were associated with the biological functions of sirtuins (Blank and Grummt, 2017; Houtkooper et al., 2012; Yamamoto et al., 2007), including gene sets of mitochondria (8.9%), epigenetics and transcription (11%), DNA repair and telomeres (9.3%), rRNA and ribosomes (7.7%), and cell cycle and replication (38.2%) (Fig. 1B). Gene sets for macromolecular diacylation, mitochondrial gene expression, histone deacetylation, and ribosome biogenesis were enriched in patients who showed short-term survival and may have developed sorafenib resistance (Fig. 1 C). Notably, all selected gene sets were reported to be downstream of SIRT7 (Barber et al., 2012; Ford et al., 2006; Kiran et al., 2015; Ryu et al., 2014a; Tong et al., 2016; Vazquez et al., 2017) (Fig. 1C). To determine whether SIRT7 expression is associated with sorafenib resistance, three independent datasets were analyzed (Fig. 1D). Although the expression of other protein deacetylases was not associated with sorafenib resistance, elevated SIRT7 expression was associated with sorafenib resistance (Fig. 1E and S1A–C). In addition, no other different sirtuin-driven integration of this expression change in sorafenib resistance cells was observed except the potential regulatory interaction partner of *SIRT7*, *SIRT1*, which was increased its expression in the resistance cells (Fig. S1D and E), presumably due to the changes in *SIRT7* expression accordingly (Fang et al., 2017). Consistently, TCGA-LIHC data indicated that SIRT7 expression was negatively correlated with the survival probability of sorafenib treated patients (Fig. 1F and G). This suggested that SIRT7 may contribute, at least in part, to sorafenib resistance.

Loss-of-SIRT7 effectively re-sensitized HCC to sorafenib

To further investigate the association between SIRT7 and sorafenib-acquired resistance, alterations in SIRT7 expression in the resistant cells were tested. A previous study showed that most HCC cell lines are intrinsically insensitive to sorafenib (Wang et al., 2018), and exposure of Huh7 and SK-Hep1 cell lines to increasing concentrations of sorafenib generated more potent sorafenib-resistant HCC sub-cell lines named Huh7^{SR} and SK-Hep1^{SR}, respectively (Fig. 1H). Sorafenib resistance was determined by the shift of the half-maximal inhibitory concentration (IC_{50}) towards a higher sorafenib concentration in all resistant cell lines than in their parental cell lines (Fig. 1I and J). The expression of SIRT7 was then analyzed together with that of a well-known biomarker for assessing the response to sorafenib, pERK1/2 (Chen et al., 2013). Interestingly, upregulated SIRT7 expression was observed together with hyperactivated pERK1/2 in both Huh7^{SR} (Fig. 2A and B) and SK-Hep1^{SR} cells (Fig. 2D and E) compared to SIRT7 expression in their parental cells. These findings suggested a negative association between SIRT7 expression and sorafenib responsiveness in HCC cells.

Based on the inverse association between SIRT7 expression and the sorafenib response, we investigated whether SIRT7 inhibition could restore sorafenib sensitivity and act synergistically with sorafenib. To address this, Huh7^{SR} and SK-Hep1^{SR} cells were transduced with the SIRT7 shRNA vector and cultured with or without sorafenib. Notably, the decreased phosphorylation of ERK1/2 was a consequence of the inhibition of SIRT7 activity in sorafenib-resistant HCC cells compared to that in their parental cells (Fig. 2C and F). Although SIRT7 knockdown alone resulted in only a modest reduction in cell viability and growth, suppression of SIRT7 expression in combination with sorafenib markedly inhibited the viability and proliferation of sorafenib-unresponsive Huh7^{SR} (Fig. 2G and H; S2A) and SK-Hep1^{SR} (Fig. 2I and J; S2B) cells. This confirmed that SIRT7 may be responsible for sorafenib-acquired resistance and that inhibition is synergistic with a low dose of sorafenib to re-sensitize HCC cells by suppressing ERK1/2 signaling.

SIRT7 inhibitors combined with sorafenib drove potent synergistic cell death by suppressing pERK1/2 signaling

To test the therapeutic potential of SIRT7 inhibition in sorafenib-resistant HCC cells, two SIRT7-targeted chemical inhibitors (SIRT7i), SIRT7i #1 and SIRT7i #2, were generated (Fig. 3A and F; S3A and B). Although both SIRT7 inhibitors attenuated cell viability when administered alone to Huh7^{SR} (Fig. 3B and G) and SK-Hep1^{SR} cells (Fig. 3C and H), potent synergistic inhibition of cell viability was observed when SIRT7i was combined with sorafenib in Huh7^{SR} (Fig. 3D and I) and SK-Hep1^{SR} cells (Fig. 3E and J). This effect was similar to that observed after *SIRT7* knockdown. In addition, the chemosensitivity of both sorafenib-resistant HCC cell lines was significantly increased by combination therapy, as measured by cell growth (Fig. 4A–D) and viability assays (Fig. S4A and B). To further confirm whether SIRT7 inhibition was responsible for suppressing ERK1/2 signaling, resistant HCC cells were treated with SIRT7i alone or in combination of SIRT7i and sorafenib. Immunoblotting revealed that inhibition of SIRT7 with a low dose of sorafenib caused a more potent and complete inhibition of ERK1/2 phosphorylation than SIRT7i alone (Fig. 4E and F). These results suggested that SIRT7 could act as a driver for the regulation of ERK1/2 signaling, which is most likely to be effective when combined with sorafenib, resulting in the suppression of ERK1/2 signaling to induce HCC cell death.

Suppression of SIRT7 inhibited tumor growth in vivo

To determine whether these in vitro findings could be confirmed in vivo, Huh7^{SR} cells were injected into immunodeficient mice. Upon tumor establishment, xenografted mice were treated with control, sorafenib, SIRT7i #1, SIRT7i #2, or their combination for 14 days (Fig. 5A).

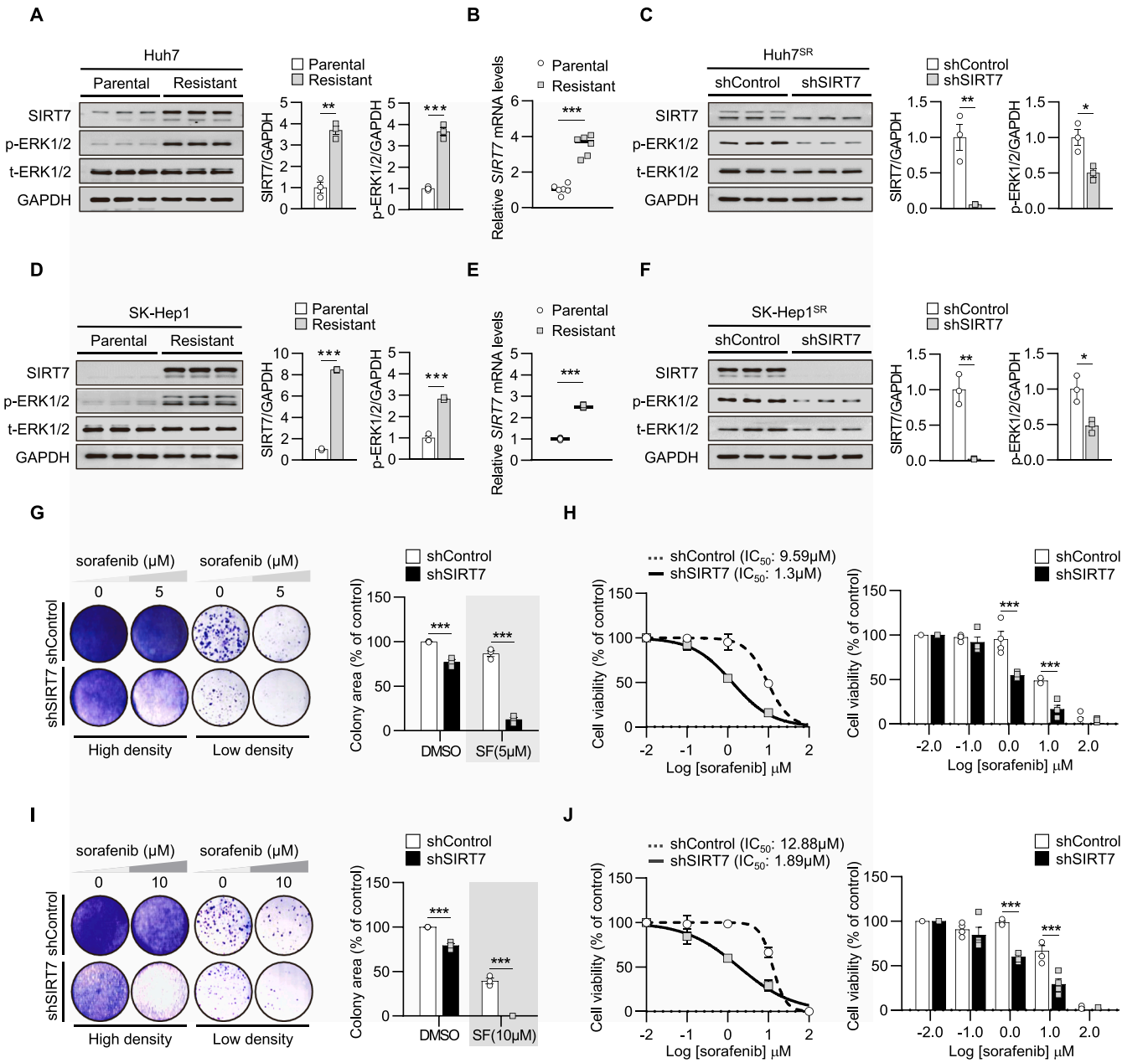

Fig. 2. SIRT7 silencing inhibits the proliferation of sorafenib-resistant liver cancer cells. (A and D) Protein expression levels of SIRT7 in Huh7^{SR} (A), SK-Hep1^{SR} (D), with their parental cells (left). SIRT7 and p-ERK1/2 levels were quantified (right). (B and E) The mRNA levels of SIRT7 in Huh7^{SR} (B) SK-Hep1^{SR} (E) with their parental cells. (C and F) *SIRT7* knockdown in Huh7^{SR} (C) and SK-Hep1^{SR} (F) was determined. SIRT7 and p-ERK1/2 levels were quantified (right). (G and I) Colony-formation assays of Huh7^{SR} (G) and SK-Hep1^{SR} cells (I) combined shRNA targeting SIRT7 with sorafenib. (H and J) Cell viability of Huh7^{SR} (K) and SK-Hep1^{SR} cells (M) upon *SIRT7* knockdown was analyzed by MTT assays. Data are represented as the mean ± SEM. Statistical analysis was conducted using a two-way ANOVA or two-tailed student's *t*-test, where appropriate, * $P < 0.05$; * * $P < 0.01$; * ** $P < 0.001$.

Photographs of the mice captured on day 14 are shown in Fig. 5C. The combination of sorafenib and two SIRT7is showed a significant synergistic effect on tumor growth rate and mass (Fig. 5D, E, and G) without affecting body weight (Fig. 5B). To support these findings, immunohistochemical staining of each tumor tissue was performed (Fig. 5F). Treatment of mice with SIRT7i alone showed moderate effects on proliferation and tumor progression. The combination treatment potently inhibited tumor proliferation and progression, as indicated by Ki-67 staining, a marker of proliferation, and AFP staining, a marker of tumor progression (Fig. 5H). Likewise, immunoblot analysis confirmed the strong suppressive effect of the combination treatment on tumor proliferation (Fig. 5I), which led to a robust reduction in ERK1/2 phosphorylation (Fig. 5J).

DDX3X was found to be a deacetylation target of SIRT7

Sirtuin enzymes regulate various metabolic processes through deacetylation of target proteins (Houtkooper et al., 2012). Therefore, the identification of their target substrates is key to understanding the functions of sirtuins. To clarify the molecular mechanism underlying the synergistic effects of SIRT7 inhibition, interactome screening was performed to identify possible SIRT7 interactors associated with ERK1/2 signaling. According to the results of the interactome analysis based on the overlap between the acetylated and MARylated proteome and the SIRT7 interactome, stress-responsive DDX3X appears to be a potent deacetylation candidate for SIRT7 (Fig. 6A and S5A). DDX3X was validated as a SIRT7 deacetylation target through reduction in

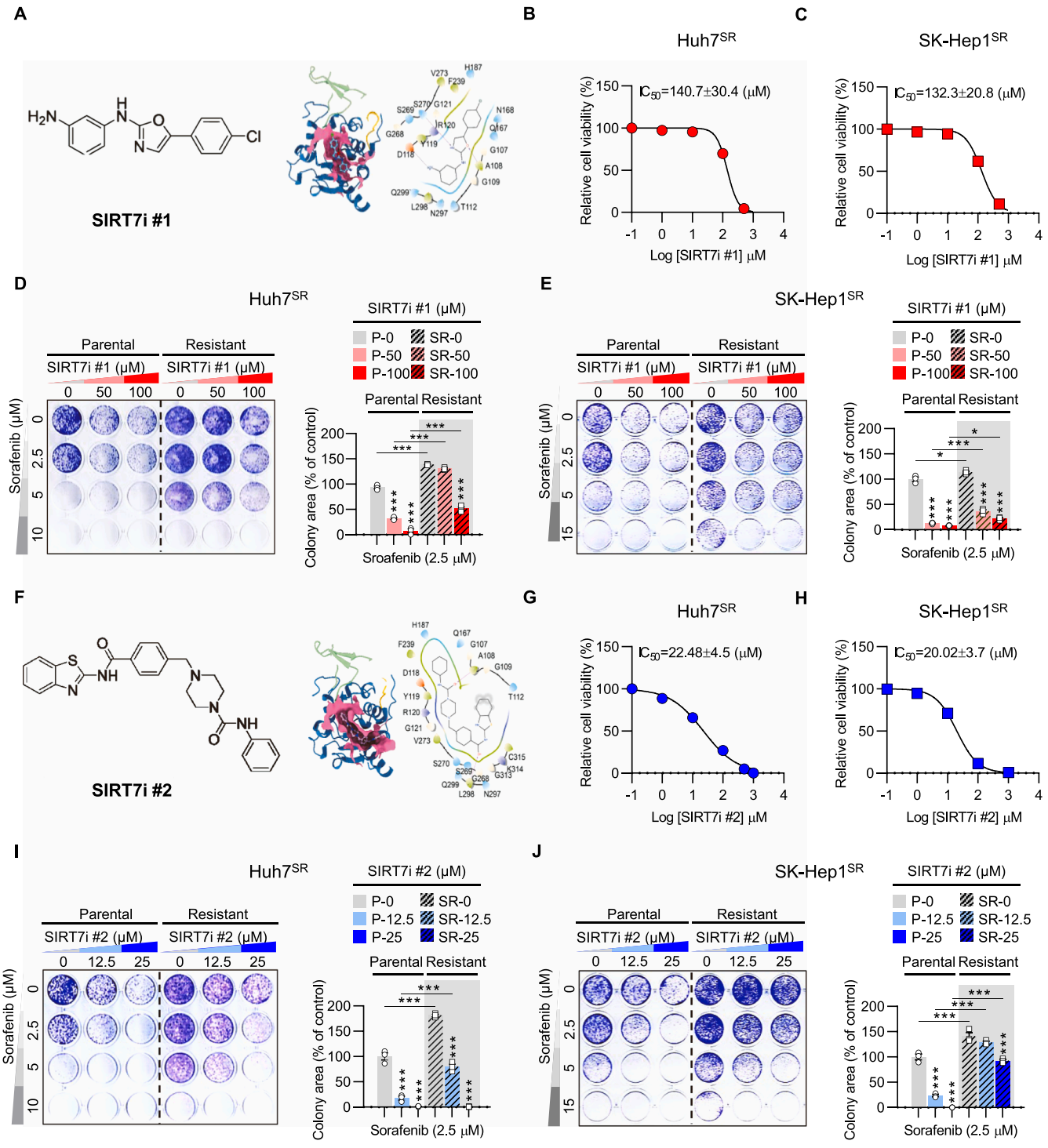

Fig. 3. Development of SIRT7-targeted chemical inhibitors. (A and F) Chemical structure and docking pose of SIRT7i #1 (A) and SIRT7i #2 (F). Schematic representation of SIRT7i #1 or SIRT7i #2 modeled structure (right). (B and C; G and H) Effect of SIRT7i #1 and SIRT7i #2 on cell viability. Both Huh7^{SR} (B and G) and SK-Hep1^{SR} cells (C and H) were treated with SIRT7i #1 or SIRT7i #2, then cell viability was determined by an MTT assay. (D and E; I and J) Long-term colony-formation assay of Huh7^{SR} (D and I) or SK-Hep1^{SR} cells (E and J) treated with sorafenib and the indicated SIRT7i #1 or SIRT7i #2. Quantification at sorafenib 2.5 μM is shown in D and E or I and J (right panel). Data are shown as the mean ± SEM. Statistical analysis was conducted using two-way ANOVA with the post-hoc two-tailed *t*-test, * $P < 0.05$; * * $P < 0.01$; * ** $P < 0.001$.

p300-induced acetylation in in vitro deacetylation assays (Fig. 6B). As a direct binding partner of SIRT7 (Fig. 6C), the level of DDX3X acetylation was analyzed by pulling down the FLAG tag in FLAG-SIRT7-overexpressing HEK293T cells, which verified that the level of acetylated DDX3X diminished upon SIRT7 overexpression (Fig. 6D). Conversely, the knockdown of endogenous *SIRT7* by transfection with an shSIRT7 vector resulted in increased levels of DDX3X pan-acetylation (Fig. 6E), confirming that DDX3X is a direct deacetylation target of SIRT7. Mass spectrometry identified the acetylated site as lysine (Lys) 55 in DDX3X (Fig. 6F). A DDX3X mutant was generated to mimic the acetylated form by replacing Lys with glutamine (K55Q) (Fig. 6G). As expected, enhanced overall acetylation was

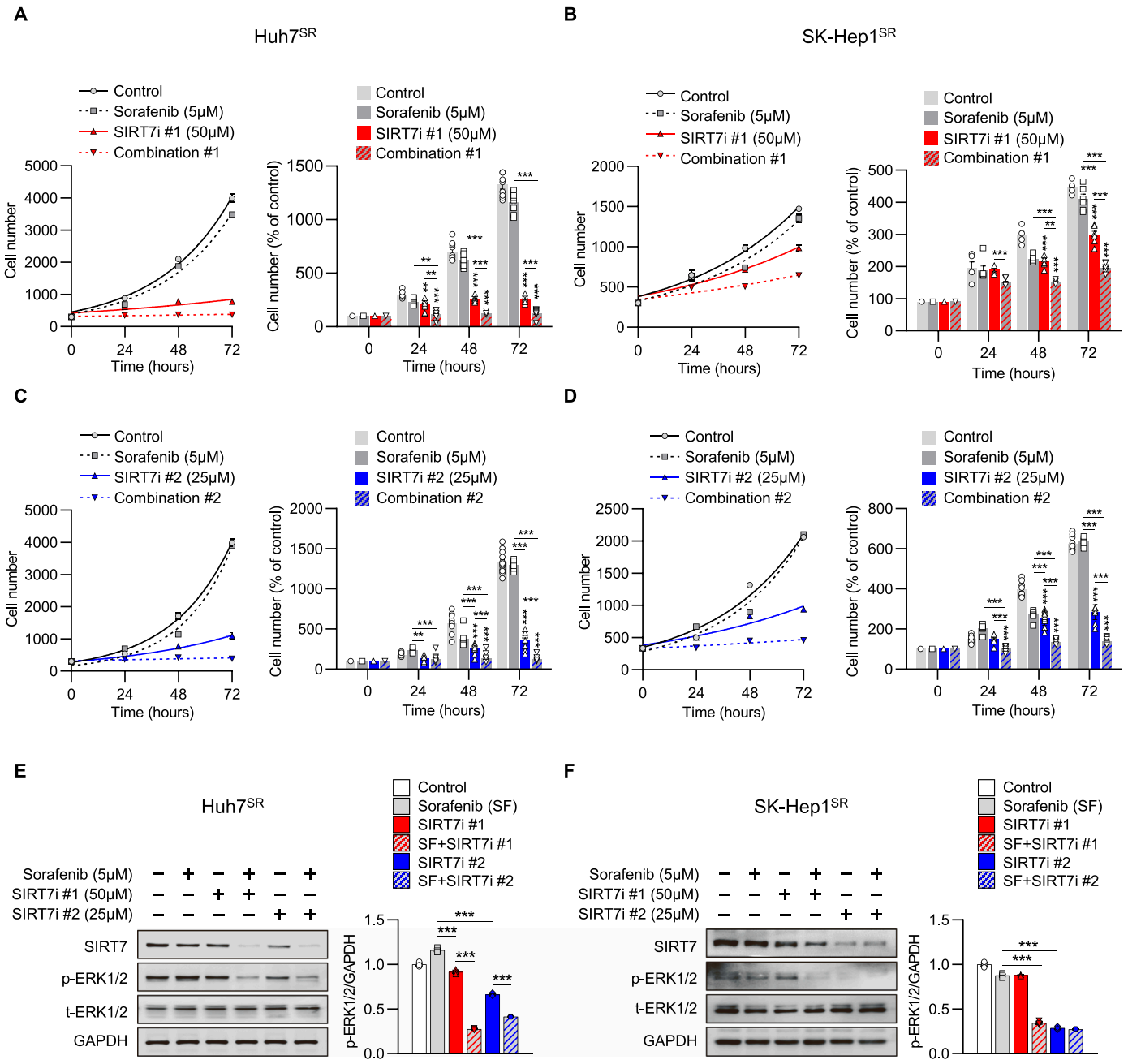

Fig. 4. Chemical inhibitor of SIRT7 sensitizes sorafenib resistance. (A and B) Numbers of Huh7^{SR} (A) and SK-Hep1^{SR} cells (B) treated with sorafenib and SIRT7i #1, either alone or their combinations, (C and D) Numbers of Huh7^{SR} (C) and SK-Hep1^{SR} cells (D) treated with sorafenib and SIRT7i #2, either alone or their combinations, were determined by trypan blue exclusion assay at the indicated days thereafter. (E and F) Huh7^{SR} (E) and SK-Hep1^{SR} cells (F) were treated with sorafenib (5 μM), SIRT7 inhibitor #1 (50 μM), SIRT7 inhibitor #2 (25 μM), or their combinations, then analyzed by western blot. The levels of pERK were also quantified (right). Data are shown as the mean ± SEM. Statistical analysis was conducted using two-way ANOVA with post-hoc two-tailed *t*-test, * $P < 0.05$; * * $P < 0.01$; * ** $P < 0.001$.

observed regardless of SIRT7 overexpression-mediated deacetylation (Fig. 6H), indicating that SIRT7-mediated deacetylation of DDX3X occurs at Lys 55.

SIRT7-mediated DDX3X modification was responsible for regulating ERK1/2 signaling

As DDX3X cellular availability is a checkpoint for cell survival decisions, we directly determined whether the stability of the DDX3X protein could also be affected by SIRT7-mediated deacetylation. SIRT7-regulated DDX3X protein stability in sorafenib-resistant HCC cells was analyzed by transfecting FLAG-SIRT7 or shSIRT7 into Huh7^{SR} and SK-Hep1^{SR} cells with cycloheximide (CHX). The half-life of endogenous DDX3X was increased by SIRT7 overexpression (Fig. 7A and C), whereas the knockdown of *SIRT7* by shRNA reversed this effect (Fig. 7B and D). To extend this finding, the ubiquitination levels of DDX3X with or without SIRT7 expression were examined. Most proteins that require initial ubiquitination and polyubiquitination of Lys residues and acetylation often share Lys residues with ubiquitination, thereby affecting the stability of the target protein (Caron et al., 2005). The ubiquitination levels of DDX3X/WT upon co-expression with FLAG-SIRT7 were lower than those in control cells (Fig. 7E), suggesting that deacetylation of

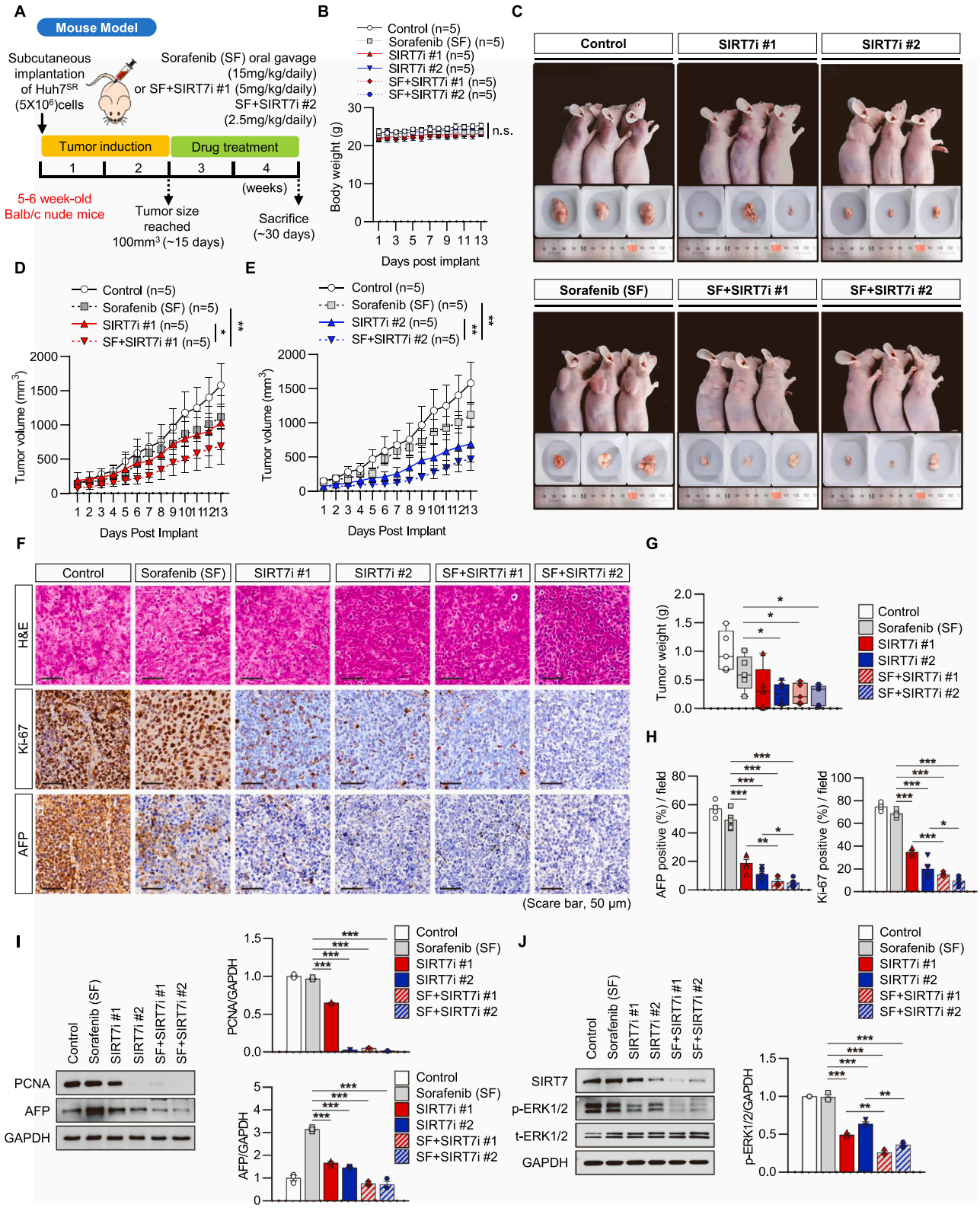

Fig. 5. Combination of SIRT7i and sorafenib displays potent antiproliferative effects in a xenograft mouse model. (A) Schematic image of the Huh7^{SR} xenografted model. After tumor establishment (~100 mm^3), mice were treated with vehicle, sorafenib, SIRT7i #1 or SIRT7i #2 plus sorafenib (n = 5 – 6). (B) Body weights of mice (g). (C) Representative photograph images of tumors formed in mice. (D and E) Tumor growth curves. SIRT7i #1 (D), SIRT7i #2 (E), or their combinations. (F) Representative images of H&E, Ki-67, and AFP staining. Scale bars, 50 μm. (G) Tumor weight (g). (H) Quantification of AFP (left) and Ki-67-positive cells (right) (n = 5). (I) Western blot analysis of PCAN and AFP levels. Each group was quantified (right). (J) SIRT7 and pERK levels in tumor tissues. Quantification of pERK (right). Data are shown as the mean ± SEM. Statistical analysis was conducted using two-way ANOVA with post-hoc two-tailed *t*-test or two-tailed student's *t*-test, where appropriate, * $P < 0.05$; * * $P < 0.01$; * ** $P < 0.001$.

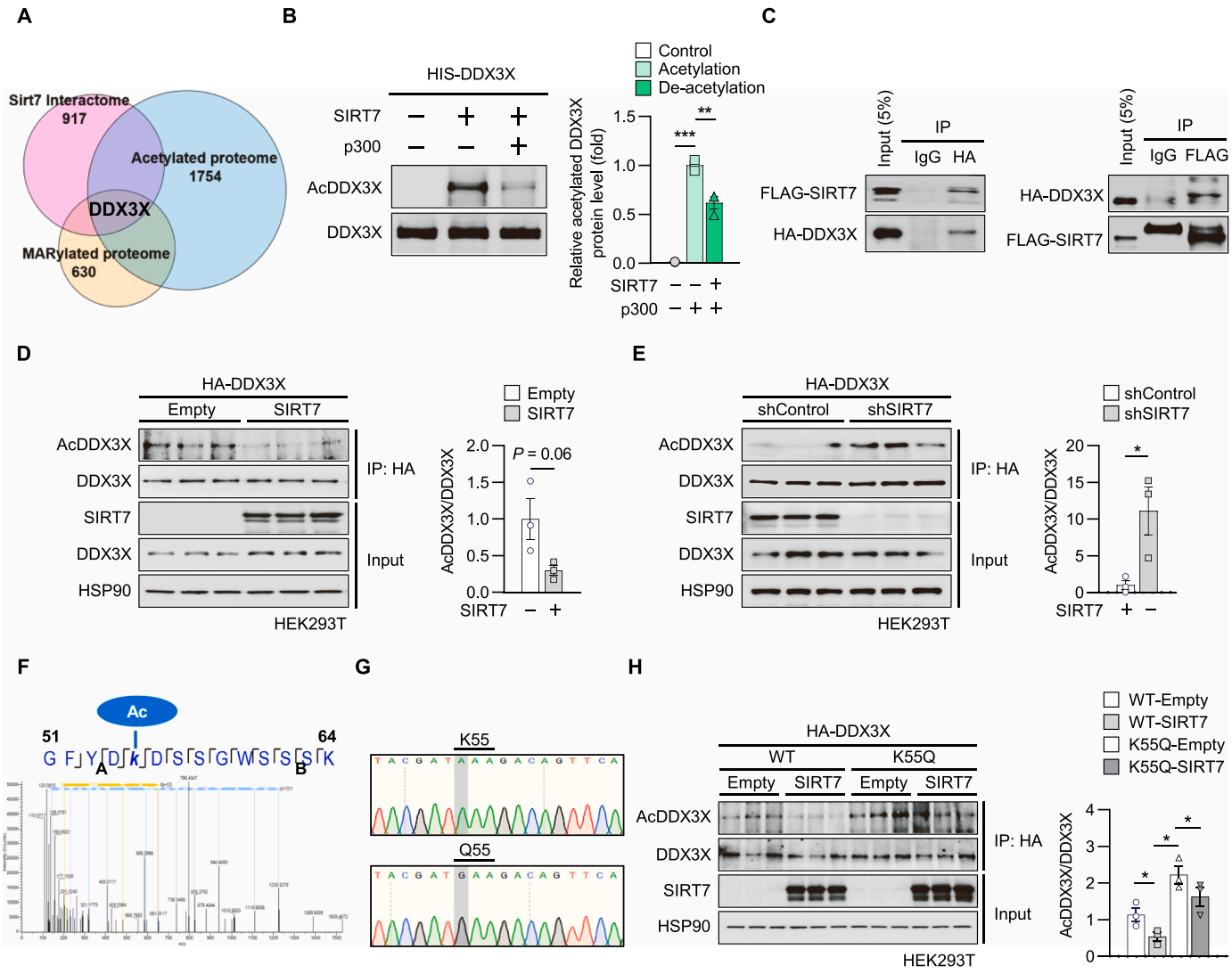

Fig. 6. DDX3X is a deacetylation target of SIRT7. (A) Venn diagram showing the integration of the acetylated, MARylated, and SIRT7 interactomes. (B) In vitro deacetylation assay of SIRT7 deacetylating DDX3X. (C) Interaction between SIRT7 and DDX3X using immunoprecipitation (IP). HEK293T cells expressing FLAG-SIRT7 with HA-DDX3X were subjected to IP analysis. (D and E) Acetylated DDX3X in SIRT7-overexpressing (D) in *SIRT7* knockdown (E) HEK293T cells. The acetylated DDX3X (AcDDX3X) level was quantified (right). (F) Nano-LC-MS/MS analysis showing SIRT7-dependent deacetylation. (G) Electropherograms of sequencing displaying the point mutant site of DDX3X. (H) Acetylation status in WT or acetylation mutant K55Q of DDX3X upon SIRT7 overexpression. AcDDX3X level was quantified (right). Data are shown as the mean ± SEM. Statistical analysis was performed by two-tailed Student's *t*-test, * $P < 0.05$; * * $P < 0.01$; * ** $P < 0.001$.

DDX3X by SIRT7 is a critical determinant of DDX3X ubiquitination. Furthermore, cells were transfected with a DDX3X acetylation mutation mimicking SIRT7 deacetylase deficiency (DDX3X/K55Q) to determine the level of DDX3X ubiquitination. As expected, DDX3X/K55Q transfected cells showed higher levels of protein degradation (Fig. 7F), indicating that K55 is a critical determinant for the ubiquitination of DDX3X. Based on the above findings, we tested whether SIRT7-mediated DDX3X modification was responsible for regulating ERK1/2 signaling and affecting the survival of sorafenib-resistant cells. Upon transfection with either DDX3X (WT) or DDX3X (K55Q) under sorafenib treatment, ERK1/2 phosphorylation was significantly decreased in DDX3X (K55Q) cells (Fig. 7G and H), and the stability of pERK1/2 was considerably decreased in K55Q cells (Fig. 7I), indicating that acetylated K55 of DDX3X suppressed ERK1/2 hyperactivation. In summary, SIRT7-mediated deacetylation of the K55 site stabilized DDX3X, and loss of SIRT7 deacetylase through acetylation of DDX3X may be required to restore sorafenib sensitivity by suppressing pERK1/2 signaling.

Loss-of-SIRT7 suppressed pERK1/2 through DDX3X-mediated NLRP3 inflammasome

Sorafenib is a potent inducer of stress granules (SGs) in HCC, and SG formation is closely associated with cell resistance to the cytotoxic effects of cellular stressors (Adjibade et al., 2015). As DDX3X plays a critical role in both SG and NLRP3 inflammasome assembly (Samir et al., 2019) and IL-1β, downstream of NLRP3 inflammasome, has been shown to activate ERK1/2 signaling (Zhang et al., 2022), it was speculated that SIRT7 activation enhances sorafenib resistance by stabilizing DDX3X protein to increase pro-survival ERK1/2 signaling by modulating both SGs and NLRP3 inflammasomes. To address this possibility, knockdown of *SIRT7* (shSIRT7) or acetylated DDX3X (K55Q) was transfected into sorafenib-resistant HCC cells, and confocal microscopy imaging of G3BP1 and NLRP3 inflammasomes was performed. Remarkably, both SG component, G3BP1, and NLRP3 signals were diminished in shSIRT7 transfected SK-Hep1^{SR} compared to those in control cells, and reduced ASC specks, an NLRP3 inflammasome component, were also observed

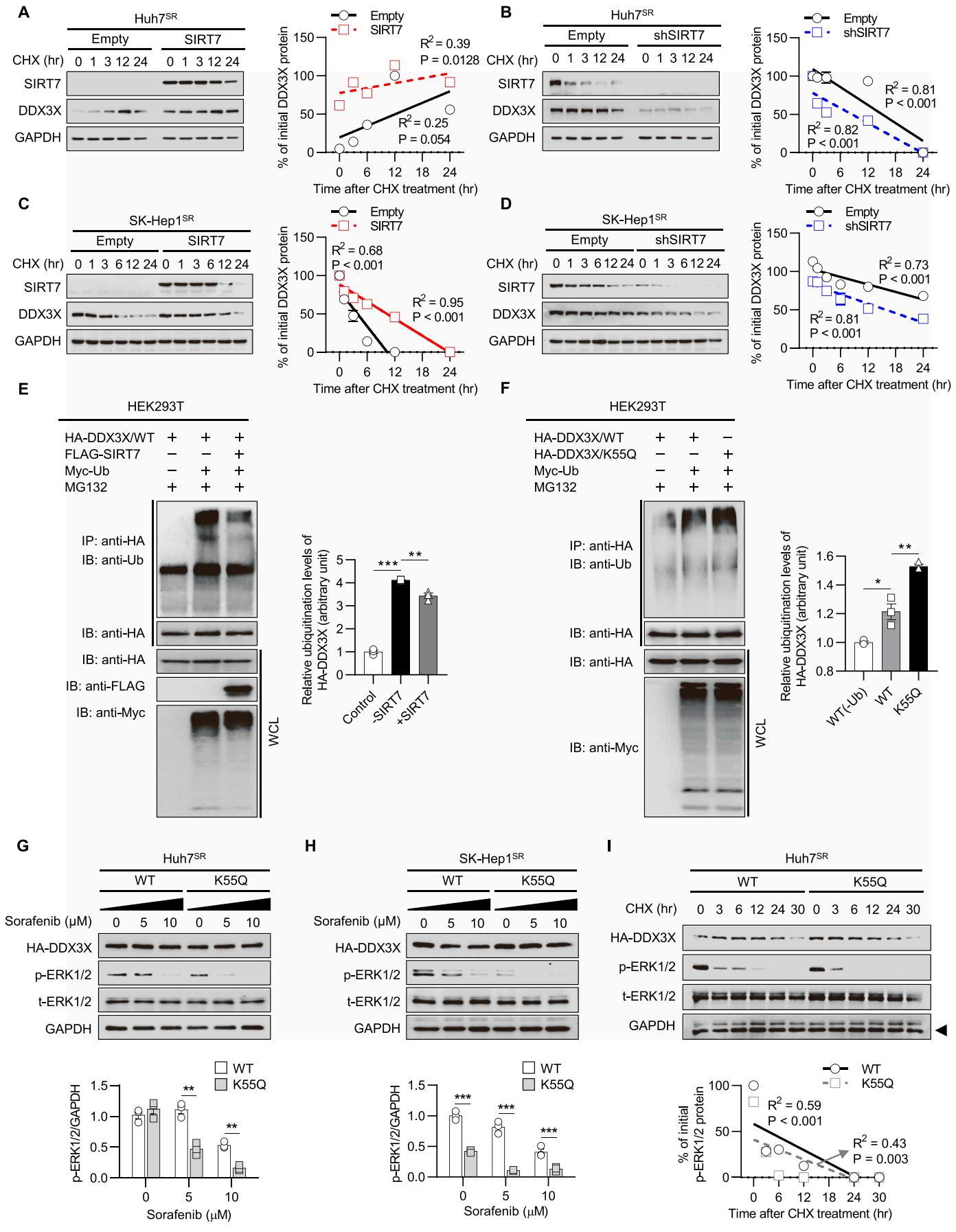

(caption on next page)

Fig. 7. SIRT7 is required to activate pERK signaling through stabilizing DDX3X. (A and C) Huh7^{SR} (A) and SK-Hep1^{SR} cells (C) were transfected with the indicated plasmids and (B and D) Huh7^{SR} (D) and SK-Hep1^{SR} cells (F) were transduced with shRNA expressing SIRT7, then treated with cycloheximide (CHX) (50 μg/mL). The percentage of initial DDX3X protein levels was analyzed (right). (E) Cells were co-transfected with Myc-Ub and HA-DDX3X/WT, FLAG-SIRT7, (F) with Myc-Ub and HA-DDX3X/WT or HA-DDX3X/K55Q, then treated with MG132. The levels of ubiquitination were quantified (right). (G and H) Huh7^{SR} (G) and SK-Hep1^{SR} cells (H) were transfected with WT or K55Q of DDX3X, then treated with sorafenib. (I) Huh7^{SR} cells were transfected with WT or K55Q of DDX3X, then treated with CHX (50 μg/mL). pERK protein levels were quantified (bottom). The data represent the means ± SEM. Statistical analysis was conducted using two-way ANOVA with post-hoc two-tailed *t*-test or two-tailed student's *t*-test, where appropriate, * $P < 0.05$; * * $P < 0.01$; * ** $P < 0.001$.

upon K55Q transfection (Fig. 8A and B). Following NLRP3 down-regulation mediated by SIRT7, the protein expression levels of caspase 1 and IL-1β also decreased significantly (Fig. 8C). To further confirmed the regulatory effect of SIRT7 inhibition on NLRP3 inflammasome, SIRT7 inhibitors treated SK-Hep1^{SR} cells and Huh7^{SR} xenografted tumor tissues were analyzed. As a result, DDX3X/NLRP3 inflammasome signaling cascade was strongly inhibited when it combined with sorafenib in vitro and in vivo which strongly supports SIRT7 mediated NLRP3 inflammasome through interaction between SIRT7 mediated DDX3X and NLRP3 (Fig. S6A-C). In addition, mRNA expression levels of IL-1β in Huh7^{SR} xenografted mice tumor tissues and its secretion levels in serum blood were further analyzed to confirm whether SIRT7 mediated inhibition of NLRP3 inflammasome suppresses accelerating tumor growth and drug resistance by disrupting the release of IL-1β (Tang et al., 2023). As we expected, inhibition of SIRT7 mediated DDX3X/NLRP3 inflammasome deactivation resulted in disrupting the release of IL1-β (Fig. S7A and B). Notably, chemical inhibition of SIRT7 decreased the gene expression levels of *IL-1β* and its downstream target, *COX2*, upon LPS stimulation in normal hepatocytes and macrophages (Fig. S8A–C) which strongly support the regulatory effect of SIRT7 on NLRP3 signaling pathway in liver cells. To further extend these findings from a clinical perspective, SK-Hep1^{SR} cells were xenografted and sorafenib treatment was applied alone or in combination with a DDX3X inhibitor (RK-33) (Fig. 8D). Without affecting the body weight of the mice (Fig. 8E), the combination treatment effectively prevented tumor growth (Fig. 8F and G). Immunohistochemical analysis of the tumors further demonstrated that sorafenib and DDX3X inhibition synergistically suppressed the progression of sorafenib-resistant HCC (Fig. 8H and I). These findings suggest the notion that SIRT7-mediated DDX3X deficiency disrupts the assembly of both SGs and NLRP3 inflammasomes to promote a pro-cell death program by suppressing ERK1/2 hyperactivation, thereby enabling cells to restore sorafenib sensitivity.

Discussion

Patients with advanced HCC are only eligible for systemic therapy, which offers marginal survival benefits owing to acquired or intrinsic chemoresistance. With increasing evidence pointing towards the crucial role of SIRT7 in tumor development, this study found that the sensitivity of acquired sorafenib resistance in HCC could be controlled by SIRT7-mediated DDX3X modification regulating ERK1/2 signaling through NLRP3 inflammasome-activated IL-1β.

Although SIRT7 is the least studied mammalian sirtuin, its fundamental roles in oncogenic transformation and tumor biology have been frequently reported (Kim et al., 2013; Paredes et al., 2014; Wang et al., 2015). In HCC, SIRT7 expression has been reported to be upregulated in a large cohort of patients with high tumor grades (Kim et al., 2013). Furthermore, Zhao et al. observed a significant increase in SIRT7 expression in most HCC tissues compared to the SIRT7 expression level in adjacent non-tumoral liver tissues (Zhao et al., 2019). In this study, SIRT7 expression was highly correlated with a poor overall survival rate in liver cancer cases and further enhanced by hyperactivated oncogenic signaling, pERK1/2, in acquired sorafenib-resistant settings. ERK1/2 reactivation in resistant cancers after prolonged treatment with RAF and MEK inhibitors has recently drawn attention (Moon and Ro, 2021). ERK1/2 activity was increased with sorafenib resistance (Fig. 2D and G), suggesting that elevated ERK1/2 phosphorylation is a predictive marker of sorafenib unresponsiveness. Moreover, hyperactive pERK1/2 was well suppressed by sorafenib combined with SIRT7 inhibitors, leading to a strong synergistic lethal effect on resistant cells. This indicates that SIRT7 acts as an oncogenic regulator of pro-survival ERK1/2 signaling, contributing to HCC progression, which is responsible for sorafenib resistance. To date, no activating modulator of pERK1/2 has been identified in sorafenib-resistant HCC cells. The results of the present study confirm the role of SIRT7 as a pro-oncogenic regulator of pERK1/2 activation, which can be a powerful predictive biomarker for assessing sorafenib resistance.

Notably, the involvement of DDX3X in activating ERK1/2 signaling pathways to promote cancer invasion has been previously demonstrated in DDX3X-overexpressing colon cancer cells (Wu et al., 2016). The increase in tumor-invasion capability induced by DDX3X was reversed by ERK1/2 inhibition. In this study, additional evidence of the decisive role of DDX3X in modulating ERK1/2 activation was found in SIRT7-deficient acetylated DDX3X in sorafenib-resistant HCC cells, which reduced ERK1/2 phosphorylation more sufficiently under a lower concentration of sorafenib (Fig. 7G and H). Therefore, the regulation of ERK1/2 signaling in sorafenib-resistant HCC cells can be controlled by SIRT7-mediated DDX3X epigenetic modifications. Mechanistically, DDX3X is required for SG and NLRP3 inflammasome assembly to enable cells to make survival decisions based on cellular availability (Samir et al., 2019). The results of the present study indicate that DDX3X deficiency, caused by the loss of SIRT7, disrupts the assembly of both SGs and NLRP3 inflammasomes, resulting in massive HCC cell death (Fig. 8A). As DDX3X has been shown to sit at the junction between inflammation and stress adaptation (Samir et al., 2019), it is possible that DDX3X acts as a cell survival checkpoint in sorafenib-resistant HCC cells.

SG assembly is a well-known cellular strategy to reduce stress-related damage and promote cell survival. Pro-tumorigenic hyperactivated signaling pathways enhance the formation of SGs, prolong the life of cancer cells, and lead to tumor cell proliferation (Asadi et al., 2021). Sorafenib has been shown to induce phosphorylation of the eIF2α (eukaryotic initiation factor 2α) to increase SG formation, and there is an absolute requirement for MEK/ERK signaling for eIF2α-mediated translational control (Thiaville et al., 2008). Thus, the inhibition of SG formation during the combination treatment may be the result of a decrease in ERK1/2 signaling. A recent study indicated that DDX3X plays a critical role in the SG-mediated inhibition of NLRP3 inflammasomes (Samir et al., 2019).

NLRP3 inflammasome consists of a scaffold protein (NLRP3), an apoptosis-associated speck-like protein containing a caspase-recruitment domain (ASC) adaptor, and caspase 1. Upon activation of NLRP3 inflammasome, caspase 1 is recruited to the platform and then autocatalytically cleaves IL-1β in the cytoplasm into mature IL-1β for its secretion (Strowig et al., 2012; Wei et al., 2014). Therefore, the primary role of the NLRP3 inflammasome is to direct inflammation when the host is in danger (Ogura et al., 2006). During liver cancer progression, activation of the NLRP3 inflammasome promotes accelerating tumor growth and metastasis through the release of IL-1β (Tang et al., 2023). The IL-1 pathway is a potent inducer of inflammation by activating and sustaining a feedback loop of pro-cell survival, which may promote drug resistance and cancer cell survival (Gelfo et al., 2020). Several studies have shown that the inhibition of NLRP3 inflammasome exerts a protective effect on inflammatory liver damage by aggravating release of IL-1β (Kim et al., 2021; Pan et al., 2021). However, the conditions under which NLRP3 inflammasomes promote cell survival in drug-resistant

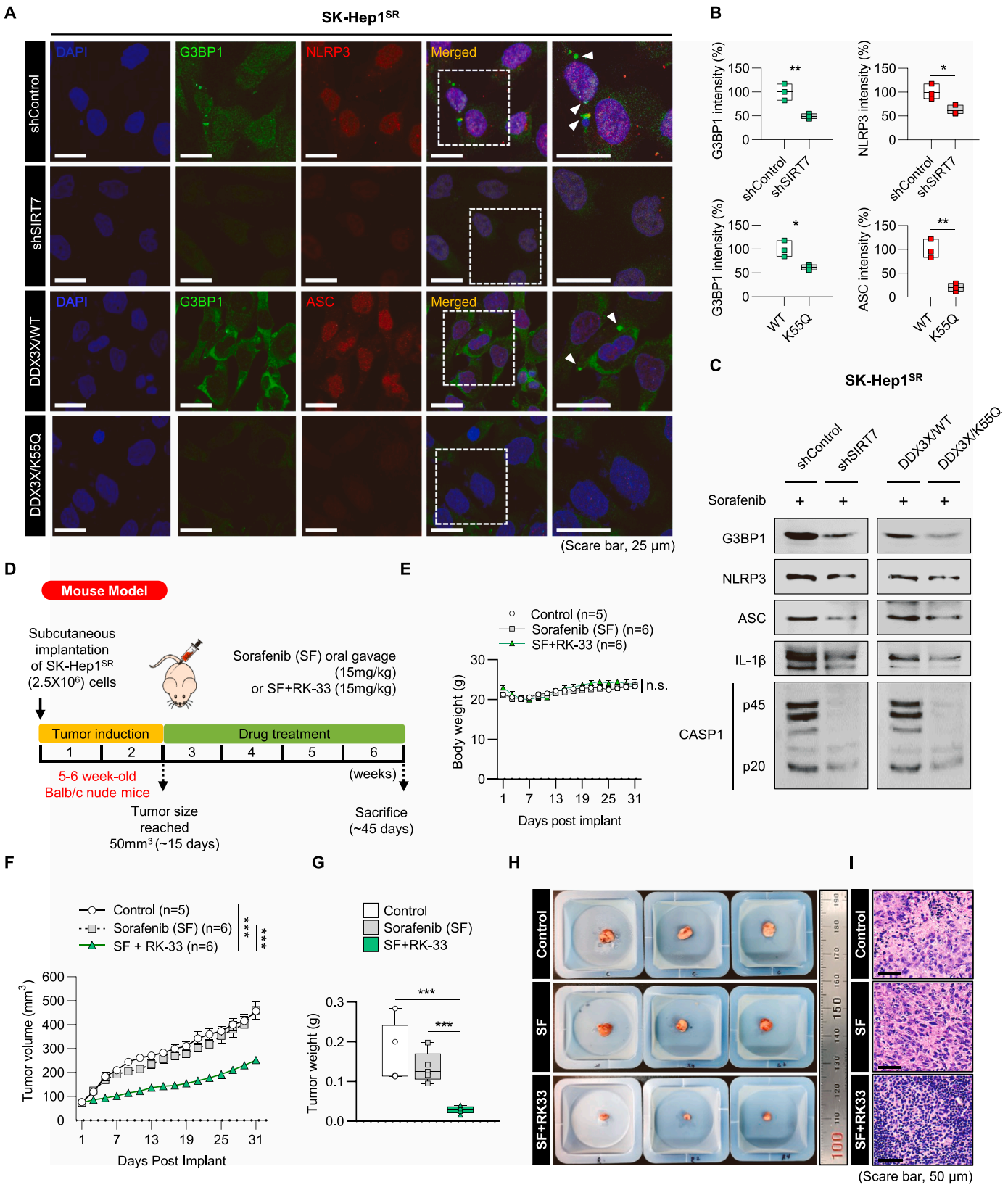

Fig. 8. Loss-of-SIRT7 inhibits NLRP3 inflammasome assembly to enable HCC cells to perform pro-survival signaling through DDX3X modification. (A and B) Confocal microscopy images of SK-Hep1^{SR} cells stained for G3BP1, NLRP3, and ASC. Scale bars, 25 μm (A). Quantification of indicated fluorescence intensities analyzed (n = 3) (B). (C) Immunoblot analysis of SGs and components of NLRP3. (D) Schematic image of the SK-Hep1^{SR} xenografted model. After tumor establishment (~50 mm^3), mice were treated with vehicle, sorafenib, or RK-33 plus sorafenib (n = 5 – 6). (E) Body weights of mice (g). (F and G) Tumor growth curves (F) and weights (g) (G). (H and I) Representative images of excised tumor (H) with H&E staining (I) from each. Scale bars, 50 μm. The data represent the means ± SEM. Statistical analysis was conducted using two-way ANOVA, * $P < 0.05$; * * $P < 0.01$; * ** $P < 0.001$.

HCC are not yet fully understood. Therefore, this study identified that DDX3X plays a critical role in the formation of NLRP3 inflammasomes in HCC. In addition, IL-1β secretion is controlled by SIRT7/DDX3X axis-regulated NLPR3 inflammasomes (Fig. 8C; S5A–C). ERK1/2 signaling is activated by various extracellular stimuli, including stress signals and inflammatory cytokines such as IL-1β (Gelfo et al., 2020; Zhang et al., 2022). Therefore, the reduction in SGs can be attributed to the suppression of ERK1/2 signaling mediated by IL-1β inhibition, and the crosstalk between SGs and NLRP3 inflammasomes can be modulated by the SIRT7/DDX3X axis in sorafenib-resistant HCC cells.

In summary, DDX3X could represent an attractive target for designing anti-HCC drugs for the therapeutic modulation of sorafenib-induced stress response by inhibiting both SG and NLRP3 inflammasome assembly and, most importantly, regulating NLRP3 inflammasome-mediated IL-1β production to control pro-survival ERK1/2 signaling to re-sensitize sorafenib resistance.

To date, only a few prognostic biomarkers of SG and NLRP3 inflammasome regulation in HCC have been identified. Thus, this study suggests that SIRT7 is a pro-oncogenic regulator of pERK1/2 hyperactivation and is a novel therapeutic biomarker for overcoming sorafenib resistance.

Financial support statement

The present study was funded by the National Research Foundation of Korea (NRF): NRF-2017K1A1A2013124, 2020R1A2C2010964, 2021R1A6A3A13044725, 2023R1A2C3006220 and RS-2023-00261370; Ecole Polytechnique Federale de Lausanne (EPFL); the European Research Council: ERC-AdG-787702; Swiss National Science Foundation: SNSF 31003A_179435; and Korea Drug Development Fund funded by Ministry of Science and ICT, Ministry of Trade, Industry, and Energy, and Ministry of Health and Welfare: RS-2023-00283539. The Korea Research Institute of Chemical Technology (KRICT) core project (grant no. kk-2431-10).

CRediT authorship contribution statement

Xu Pan: Data curation, Project administration, Resources. **Ryu Dongryeol:** Conceptualization, Data curation, Formal analysis, Funding acquisition, Project administration, Resources, Software, Supervision, Validation, Visualization, Writing – review & editing. **Kim Yun Hak:** Data curation, Formal analysis, Investigation, Resources, Software. **Jo Yunju:** Data curation, Formal analysis, Investigation, Software, Validation, Visualization. **Kang Baeki E.:** Formal analysis, Investigation, Methodology, Resources, Software, Validation, Visualization. **Kwon Jeongho:** Conceptualization, Resources. **Pandit Navin:** Investigation, Resources, Validation. **Gariani Joanna:** Conceptualization, Resources, Supervision. **Gariani Karim:** Conceptualization, Project administration, Resources, Supervision. **Auwerx Johan:** Conceptualization, Project administration, Resources, Supervision, Writing – original draft, Writing – review & editing. **Schoonjans Kristina:** Conceptualization, Project administration, Supervision. **Kim Yuna:** Conceptualization, Data curation, Formal analysis, Investigation, Methodology, Resources, Software, Validation, Visualization, Writing – original draft, Writing – review & editing. **Kim Kwang Rok:** Funding acquisition, Project administration, Resources, Supervision. **Jung Kwan-Young:** Formal analysis, Investigation, Resources, Validation, Visualization, Writing – review & editing. **Ha Ki-Tae:** Conceptualization, Resources, Supervision, Validation. **Bae Sung-Jin:** Conceptualization, Resources, Supervision. **Shong Minho:** Conceptualization, Project administration, Resources, Supervision. **Yi Hyon-Seung:** Conceptualization, Resources, Supervision. **Kim Doyoun:** Data curation, Formal analysis, Investigation, Software, Validation, Visualization. **Kim Kyun-Hwan:** Conceptualization, Resources, Supervision. **Lee Chang-Woo:** Conceptualization, Funding acquisition, Project administration, Resources, Supervision, Writing – review & editing. **Jung Hee Jung:** Data curation, Formal analysis, Resources, Software, Supervision, Validation. **Nam Seungyoon:** Conceptualization, Resources, Software, Supervision. **Verbeek Jef:** Conceptualization, Supervision, Writing – review & editing. **Lee Junguee:** Conceptualization, Resources, Supervision.

Declaration of Competing Interest

The authors declare that they have no known competing financial interests or personal relationships that could have appeared to influence the work reported in this paper.

Acknowledgements

We would like to thank everyone who participated in this study.

Appendix A. Supporting information

Supplementary data associated with this article can be found in the online version at doi:10.1016/j.drup.2024.101054.

References

Adjibade, P., St-Sauveur, V.G., Quevillon Huberdeau, M., Fournier, M.J., Savard, A., Coudert, L., Khandjian, E.W., Mazroui, R., 2015. Sorafenib, a multikinase inhibitor, induces formation of stress granules in hepatocarcinoma cells. Oncotarget 6, 43927–43943.

Asadi, M.R., Rahmanpour, D., Moslehian, M.S., Sabaie, H., Hassani, M., Ghafouri-Fard, S., Taheri, M., Rezazadeh, M., 2021. Stress granules involved in formation, progression and metastasis of cancer: a scoping review. Front Cell Dev. Biol. 9, 745394.

Barber, M.F., Michishita-Kioi, E., Xi, Y., Tasselli, L., Kioi, M., Moqtaderi, Z., Tennen, R.I., Paredes, S., Young, N.L., Chen, K., Struhl, K., Garcia, B.A., Gozani, O., Li, W., Chua, K.F., 2012. SIRT7 links H3K18 deacetylation to maintenance of oncogenic transformation. Nature 487, 114–118.

Blank, M.F., Grummt, I., 2017. The seven faces of SIRT7. Transcription 8, 67–74.

Bray, F., Ferlay, J., Soerjomataram, I., Siegel, R.L., Torre, L.A., Jemal, A., 2018. Global cancer statistics 2018: GLOBOCAN estimates of incidence and mortality worldwide for 36 cancers in 185 countries. CA A Cancer J. Clin. 68, 394–424.

Bruix, J., Chan, S.L., Galle, P.R., Rimassa, L., Sangro, B., 2021. Systemic treatment of hepatocellular carcinoma: an EASL position paper. J. Hepatol. 75, 960–974.

Byun, J.K., Lee, S., Kang, G.W., Lee, Y.R., Park, S.Y., Song, I.S., Yun, J.W., Lee, J., Choi, Y. K., Park, K.G., 2022. Macropinocytosis is an alternative pathway of cysteine acquisition and mitigates sorafenib-induced ferroptosis in hepatocellular carcinoma. J. Exp. Clin. Cancer Res. 41, 98.

Caron, C., Boyault, C., Khochbin, S., 2005. Regulatory cross-talk between lysine acetylation and ubiquitination: role in the control of protein stability. Bioessays 27, 408–415.

Chen, D., Zhao, P., Li, S.Q., Xiao, W.K., Yin, X.Y., Peng, B.G., Liang, L.J., 2013. Prognostic impact of pERK in advanced hepatocellular carcinoma patients treated with sorafenib. Eur. J. Surg. Oncol. 39.

Fang, J., Ianni, A., Smolka, C., Vakhrusheva, O., Nolte, H., Kruger, M., Wietelmann, A., Simonet, N.G., Adrian-Segarra, J.M., Vaquero, A., Braun, T., Bober, E., 2017. Sirt7 promotes adipogenesis in the mouse by inhibiting autocatalytic activation of Sirt1. Proc. Natl. Acad. Sci. USA 114, E8352–E8361.

Finn, R.S., Qin, S., Ikeda, M., Galle, P.R., Ducreux, M., Kim, T.Y., Kudo, M., Breder, V., Merle, P., Kaseb, A.O., Li, D., Verret, W., Xu, D.Z., Hernandez, S., Liu, J., Huang, C., Mulla, S., Wang, Y., Lim, H.Y., Zhu, A.X., Cheng, A.L., Investigators, I.M., 2020. Atezolizumab plus Bevacizumab in unresectable hepatocellular carcinoma. N. Engl. J. Med. 382, 1894–1905.

Ford, E., Voit, R., Liszt, G., Magin, C., Grummt, I., Guarente, L., 2006. Mammalian Sir2 homolog SIRT7 is an activator of RNA polymerase I transcription. Genes Dev. 20, 1075–1080.

Fukuda, M., Yoshizawa, T., Karim, M.F., Sobuz, S.U., Korogi, W., Kobayasi, D., Okanishi, H., Tasaki, M., Ono, K., Sawa, T., Sato, Y., Chirifu, M., Masuda, T., Nakamura, T., Tanoue, H., Nakashima, K., Kobashigawa, Y., Morioka, H., Bober, E., Ohtsuki, S., Yamagata, Y., Ando, Y., Oike, Y., Araki, N., Takeda, S., Mizuta, H., Yamagata, K., 2018. SIRT7 has a critical role in bone formation by regulating lysine acylation of SP7/Osterix. Nat. Commun. 9.

Gelfo, V., Romaniello, D., Mazzeschi, M., Sgarzi, M., Grilli, G., Morselli, A., Manzan, B., Rihawi, K., Lauriola, M., 2020. Roles of IL-1 in cancer: from tumor progression to resistance to targeted therapies. Int J. Mol. Sci. 21.

Gong, J., Wang, H., Lou, W., Wang, G., Tao, H., Wen, H., Liu, Y., Xie, Q., 2018. Associations of sirtuins with clinicopathological parameters and prognosis in non–small cell lung cancer. Cancer Manag. Res. 10.

Houtkooper, R.H., Pirinen, E., Auwerx, J., 2012. Sirtuins as regulators of metabolism and healthspan. Nat. Rev. Mol. Cell Bio 13, 225–238.

Ianni, A., Kumari, P., Tarighi, S., Simonet, N.G., Popescu, D., Guenther, S., Holper, S., Schmidt, A., Smolka, C., Yue, S., Kruger, M., Fiorillo, C., Vaquero, A., Bober, E.,

Braun, T., 2021. SIRT7-dependent deacetylation of NPM promotes p53 stabilization following UV-induced genotoxic stress. Proc. Natl. Acad. Sci. USA 118.
Kim, H.Y., Choi, Y.J., Kim, S.K., Kim, H., Jun, D.W., Yoon, K., Kim, N., Hwang, J., Kim, Y. M., Lim, S.C., Kang, K.W., 2021. Auranofin prevents liver fibrosis by system Xc-mediated inhibition of NLRP3 inflammasome. Commun. Biol. 4, 824.
Kim, J.H., Kim, D., Cho, S.J., Jung, K.Y., Kim, J.H., Lee, J.M., Jung, H.J., Kim, K.R., 2019. Identification of a novel SIRT7 inhibitor as anticancer drug candidate. Biochem. Biophys. Res. Commun. 508.
Kim, J.K., Noh, J.H., Jung, K.H., Eun, J.W., Bae, H.J., Kim, M.G., Chang, Y.G., Shen, Q., Park, W.S., Lee, J.Y., Borlak, J., Nam, S.W., 2013. Sirtuin7 oncogenic potential in human hepatocellular carcinoma and its regulation by the tumor suppressors MiR-125a-5p and MiR-125b. Hepatology 57, 1055–1067.
Kiran, S., Anwar, T., Kiran, M., Ramakrishna, G., 2015. Sirtuin 7 in cell proliferation, stress and disease: rise of the Seventh Sirtuin! Cell Signal 27, 673–682.
Liu, Y., Xun, Z., Ma, K., Liang, S., Li, X., Zhou, S., Sun, L., Liu, Y., Du, Y., Guo, X., Cui, T., Zhou, H., Wang, J., Yin, D., Song, R., Zhang, S., Cai, W., Meng, F., Guo, H., Zhang, B., Yang, D., Bao, R., Hu, Q., Wang, J., Ye, Y., Liu, L., 2023. Identification of a tumour immune barrier in the HCC microenvironment that determines the efficacy of immunotherapy. J. Hepatol. 78, 770–782.
Li, W., Sun, Z., Chen, C., Wang, L., Geng, Z., Tao, J., 2018. Sirtuin7 has an oncogenic potential via promoting the growth of cholangiocarcinoma cells. Biomed. Pharmacother. 100.
Llovet, J.M., Peña, C.E.A., Lathia, C.D., Shan, M., Meinhardt, G., Bruix, J., 2012. Plasma biomarkers as predictors of outcome in patients with advanced hepatocellular carcinoma. Clin. Cancer Res. 18.
Llovet, J.M., Ricci, S., Mazzaferro, V., Hilgard, P., Gane, E., Blanc, J.F., de Oliveira, A.C., Santoro, A., Raoul, J.L., Forner, A., Schwartz, M., Porta, C., Zeuzem, S., Bolondi, L., Greten, T.F., Galle, P.R., Seitz, J.F., Borbath, I., Haussinger, D., Giannaris, T., Shan, M., Moscovici, M., Voliotis, D., Bruix, J., Group, S.I.S., 2008. Sorafenib in advanced hepatocellular carcinoma. N. Engl. J. Med 359, 378–390.
Moon, H., Ro, S.W., 2021. MAPK/ERK signaling pathway in hepatocellular carcinoma. Cancers 13.
Negri, F.V., Dal Bello, B., Porta, C., Campanini, N., Rossi, S., Tinelli, C., Poggi, G., Missale, G., Fanello, S., Salvagni, S., Ardizzoni, A., Maria, S.E., 2015. Expression of pERK and VEGFR-2 in advanced hepatocellular carcinoma and resistance to sorafenib treatment. Liver Int. 35.
Ogura, Y., Sutterwala, F.S., Flavell, R.A., 2006. The inflammasome: first line of the immune response to cell stress. Cell 126, 659–662.
Pan, M.X., Zheng, C.Y., Deng, Y.J., Tang, K.R., Nie, H., Xie, J.Q., Liu, D.D., Tu, G.F., Yang, Q.H., Zhang, Y.P., 2021. Hepatic protective effects of Shenling Baizhu powder, a herbal compound, against inflammatory damage via TLR4/NLRP3 signalling pathway in rats with nonalcoholic fatty liver disease. J. Integr. Med 19, 428–438.
Paredes, S., Villanova, L., Chua, K.F., 2014. Molecular pathways: emerging roles of mammalian Sirtuin SIRT7 in cancer. Clin. Cancer Res. 20.
Park, E.S., Byun, Y.H., Park, S., Jang, Y.H., Han, W.R., Won, J., Cho, K.C., Kim, D.H., Lee, A.R., Shin, G.C., Park, Y.K., Kang, H.S., Sim, H., Ha, Y.N., Jae, B., Son, A., Kim, P., Yu, J., Lee, H.M., Kwon, S.B., Kim, K.P., Lee, S.H., Park, Y.M., Seong, B.L., Kim, K.H., 2019. Co-degradation of interferon signaling factor DDX3 by PB1-F2 as a basis for high virulence of 1918 pandemic influenza. EMBO J. 38.
Personeni, N., Rimassa, L., Pressiani, T., Destro, A., Ligorio, C., Tronconi, M.C., Bozzarelli, S., Carnaghi, C., Di Tommaso, L., Giordano, L., Roncalli, M., Santoro, A., 2013. Molecular determinants of outcome in sorafenib-treated patients with hepatocellular carcinoma. J. Cancer Res. Clin. Oncol.
Picard, M., Do, Why, 2022. We care more about disease than health? Phenomics 2, 145–155.
Pina, R., Santos-Diaz, A.I., Orta-Salazar, E., Aguilar-Vazquez, A.R., Mantellero, C.A., Acosta-Galeana, I., Estrada-Mondragon, A., Prior-Gonzalez, M., Martinez-Cruz, J.I., Rosas-Arellano, A., 2022. Ten approaches that improve immunostaining: a review of the latest advances for the optimization of immunofluorescence. Int J. Mol. Sci. 23.
Reddy, K.B., Nabha, S.M., Atanaskova, N., 2003. Role of MAP kinase in tumor progression and invasion. Cancer Metastas. Rev. 22.
Rothgiesser, K.M., Erener, S., Waibel, S., Lüscher, B., Hottiger, M.O., 2010. SIRT2 regulates NF-κB-dependent gene expression through deacetylation of p65 Lys310. J. Cell Sci. 123.
Ryu, D., Jo, Y.S., Lo Sasso, G., Stein, S., Zhang, H., Perino, A., Lee, J.U., Zeviani, M., Romand, R., Hottiger, M.O., Schoonjans, K., Auwerx, J., 2014a. A SIRT7-dependent acetylation switch of GABPbeta1 controls mitochondrial function. Cell Metab. 20, 856–869.
Ryu, D., Jo, Y.S., Lo Sasso, G., Stein, S., Zhang, H., Perino, A., Lee, J.U., Zeviani, M., Romand, R., Hottiger, M.O., Schoonjans, K., Auwerx, J., 2014b. A SIRT7-dependent acetylation switch of GABPβ1 controls mitochondrial function. Cell Metab. 20.
Samir, P., Kesavardhana, S., Patmore, D.M., Gingras, S., Malireddi, R.K.S., Karki, R., Guy, C.S., Briard, B., Place, D.E., Bhattacharya, A., Sharma, B.R., Nourse, A., King, S. V., Pitre, A., Burton, A.R., Pelletier, S., Gilbertson, R.J., Kanneganti, T.D., 2019. DDX3X acts as a live-or-die checkpoint in stressed cells by regulating NLRP3 inflammasome. Nature 573, 590–594.
Shigeta, K., Matsui, A., Kikuchi, H., Klein, S., Mamessier, E., Chen, I.X., Aoki, S., Kitahara, S., Inoue, K., Shigeta, A., Hato, T., Ramjiawan, R.R., Staiculescu, D., Zopf, D., Fiebig, L., Hobbs, G.S., Quaas, A., Dima, S., Popescu, I., Huang, P., Munn, L. L., Cobbold, M., Goyal, L., Zhu, A.X., Jain, R.K., Duda, D.G., 2020. Regorafenib combined with PD1 blockade increases CD8 T-cell infiltration by inducing CXCL10 expression in hepatocellular carcinoma. J. Immunother. Cancer 8.
Siegel, R.L., Miller, K.D., Jemal, A., 2019. Cancer statistics, 2019. CA A Cancer J. Clin. 69, 7–34.
Strowig, T., Henao-Mejia, J., Elinav, E., Flavell, R., 2012. Inflammasomes in health and disease. Nature 481, 278–286.
Tang, Y.L., Tao, Y., Zhu, L., Shen, J.L., Cheng, H., 2023. Role of NLRP3 inflammasome in hepatocellular carcinoma: a double-edged sword. Int Immunopharmacol. 118, 110107.
Thiaville, M.M., Pan, Y.X., Gjymishka, A., Zhong, C., Kaufman, R.J., Kilberg, M.S., 2008. MEK signaling is required for phosphorylation of eIF2alpha following amino acid limitation of HepG2 human hepatoma cells. J. Biol. Chem. 283, 10848–10857.
Tong, Z., Wang, Y., Zhang, X., Kim, D.D., Sadhukhan, S., Hao, Q., Lin, H., 2016. SIRT7 is activated by DNA and deacetylates histone H3 in the chromatin context. ACS Chem. Biol. 11, 742–747.
Vakhrusheva, O., Smolka, C., Gajawada, P., Kostin, S., Boettger, T., Kubin, T., Braun, T., Bober, E., 2008. Sirt7 increases stress resistance of cardiomyocytes and prevents apoptosis and inflammatory cardiomyopathy in mice. Circ. Res. 102, 703–710.
Vazquez, B.N., Thackray, J.K., Serrano, L., 2017. Sirtuins and DNA damage repair: SIRT7 comes to play. Nucleus 8, 107–115.
Wang, C., Jin, H., Gao, D., Lieftink, C., Evers, B., Jin, G., Xue, Z., Wang, L., Beijersbergen, R.L., Qin, W., Bernards, R., 2018. Phospho-ERK is a biomarker of response to a synthetic lethal drug combination of sorafenib and MEK inhibition in liver cancer. J. Hepatol. 69, 1057–1065.
Wang, H.L., Lu, R.Q., Xie, S.H., Zheng, H., Wen, X.M., Gao, X., Guo, L., 2015. SIRT7 exhibits oncogenic potential in human ovarian cancer cells. Asian Pac. J. Cancer Prev.
Wei, W., Jing, Z.X., Ke, Z., Yi, P., 2017. Sirtuin 7 plays an oncogenic role in human osteosarcoma via downregulating CDC4 expression. Am. J. Cancer Res. 7.
Wei, Q., Mu, K., Li, T., Zhang, Y., Yang, Z., Jia, X., Zhao, W., Huai, W., Guo, P., Han, L., 2014. Deregulation of the NLRP3 inflammasome in hepatic parenchymal cells during liver cancer progression. Lab Invest 94, 52–62.
Wu, D.W., Lin, P.L., Cheng, Y.W., Huang, C.C., Wang, L., Lee, H., 2016. DDX3 enhances oncogenic KRAS-induced tumor invasion in colorectal cancer via the β-catenin/ZEB1 axis. Oncotarget 7.
Yamamoto, H., Schoonjans, K., Auwerx, J., 2007. Sirtuin functions in health and disease. Mol. Endocrinol. 21, 1745–1755.
Yang, C., Zhang, H., Zhang, L., Zhu, A.X., Bernards, R., Qin, W., Wang, C., 2023. Evolving therapeutic landscape of advanced hepatocellular carcinoma. Nat. Rev. Gastroenterol. Hepatol. 20, 203–222.
Yu, H., Ye, W., Wu, J., Meng, X., Liu, R.Y., Ying, X., Zhou, Y., Wang, H., Pan, C., Huang, W., 2014. Overexpression of Sirt7 exhibits oncogenic property and serves as a prognostic factor in colorectal cancer. Clin. Cancer Res. 20.
Zhang, J., Wang, L., Liu, Y., Liu, W., Ma, Z., 2022. Exogenous interleukin-1 beta promotes the proliferation and migration of HeLa cells via the MEK/ERK signaling pathway. Mol. Biol. Rep. 49, 3765–3772.
Zhang, Z., Zhou, X., Shen, H., Wang, D., 2009. Phosphorylated ERK is a potential predictor of sensitivity to sorafenib when treating hepatocellular carcinoma: evidence from an in vitro study. BMC Med. 7.
Zhao, J., Wozniak, A., Adams, A., Cox, J., Vittal, A., Voss, J., Bridges, B., Weinman, S.A., Li, Z., 2019. SIRT7 regulates hepatocellular carcinoma response to therapy by altering the p53-dependent cell death pathway. J. Exp. Clin. Cancer Res. CR 38.
Zhao, J., Xu, H., Su, Y., Pan, J., Xie, S., Xu, J., Qin, L., 2023. Emerging regulatory mechanisms of N(6)-methyladenosine modification in cancer metastasis. Phenomics 3, 83–100.